EUROPEAN ORGANIZATION FOR NUCLEAR RESEARCH

CERN-PPE/93-103
4 May 1993

RADIATIVE PROTONIUM ANNIHILATION INTO $\gamma\gamma$, $\gamma\pi^0$, $\gamma\eta$, $\gamma\omega$, AND $\gamma\eta'$

The Crystal Barrel Collaboration

C. Amsler[13], D.S. Armstrong[1], I. Augustin[7], C.A. Baker[4], B.M. Barnett[10], C.J. Batty[4], K. Beuchert[2], P. Birien[1], J. Bistirlich[1], P. Blüm[7], R. Bossingham[1], H. Bossy[1], K. Braune[11], J. Brose[10], D.V. Bugg[8], M. Burchell[5], T. Case[1], S.U. Chung[10,a], A. Cooper[8], K.M. Crowe[1], H.P. Dietz[11], S. v. Dombrowski[13], M. Doser[5], W. Dünnweber[11], D. Engelhardt[7], M. Englert[11,f], M.A. Faessler[11], C. Felix[11], G. Folger[11], R. Hackmann[10], R.P. Haddock[9], F.H. Heinsius[6], N.P. Hessey[5], P. Hidas[3], P. Illinger[11], D. Jamnik[11,b], Z. Jávorfi[3], H. Kalinowsky[10], B. Kämmle[6], T. Kiel[6], J. Kisiel[11,c], E. Klempt[10], M. Kobel[5], H. Koch[2], C. Kolo[11], K. Königsmann[11,d], M. Kunze[2], R. Landua[5], J. Lüdemann[2], H. Matthaey[2], M. Merkel[10], J.P. Merlo[10], C.A. Meyer[13], L. Montanet[5], A. Noble[13], F. Ould-Saada[13], K. Peters[2], G. Pinter[3], S. Ravndal[2], J. Salk[2], A.H. Sanjari[8,e], E. Schäfer[10], B. Schmid[13], P. Schmidt[6], S. Spanier[10], C. Straßburger[10], U. Strohbusch[6], M. Suffert[12], D. Urner[13], C. Völcker[11], F. Walter[10], D. Walther[2], S. Waßmer[7], U. Wiedner[6], N. Winter[7], J. Zoll[5], Č. Zupančič[11].

Submitted to Phys. Lett. B

---

1) University of California, LBL, Berkeley, CA 94720, USA.

2) Universität Bochum, D-4630 Bochum, Germany.

3) Academy of Science, H-1525 Budapest, Hungary.

4) Rutherford Appleton Laboratory, Chilton, Didcot OX110QX, UK.

5) CERN, CH-1211 Genève, Switzerland.

6) Universität Hamburg, D-2000 Hamburg, Germany.

7) Universität Karlsruhe, D-7500 Karlsruhe, Germany.

8) Queen Mary and Westfield College, London E1 4NS, UK.

9) University of California, Los Angeles, CA 90024, USA.

10) Universität Mainz, D-6500 Mainz, Germany.

11) Universität München, D-8000 München, Germany.

12) Centre de Recherches Nucléaires, F-67037 Strasbourg, France.

13) Universität Zürich, CH-8001 Zürich, Switzerland.

a) On leave of absence from BNL, Upton, NY, USA.

b) On leave of absence from the University of Ljubljana, Ljubljana, Slovenia.

c) On leave of absence from the University of Silesia, Katowice, Poland.

d) Now at Max-Planck-Institut, D-6900 Heidelberg, Germany.

e) Now at State University of Stony Brook, Stony Brook, NY, USA.

f) This work is part of the Ph.D. thesis of M. Englert.

Abstract

Radiative $p\bar{p}$ annihilation at rest into $\gamma\gamma$, $\gamma\pi^0$, $\gamma\eta$, $\gamma\omega$, and $\gamma\eta'$ has been measured with the Crystal Barrel detector at LEAR for antiprotons stopped in liquid hydrogen. The branching ratios are $BR_{\gamma\pi^0} = (44 \pm 4) \times 10^{-6}$, $BR_{\gamma\eta} = (9.3 \pm 1.4) \times 10^{-6}$, and $BR_{\gamma\omega} = (68 \pm 19) \times 10^{-6}$, respectively. For $BR_{\gamma\gamma}$ and $BR_{\gamma\eta'}$ we find new upper limits of 0.63×10^{-6} and 12×10^{-6} (95% confidence level), respectively.

Proton–antiproton annihilation at rest leads to a rich variety of final states. The more complex final states provide a promising environment for meson spectroscopy including the search for exotic mesons such as glueballs and hybrids. The less complex two-body final states are best suited for a study of annihilation dynamics. Among them, the simplest contain two elementary particles ($\gamma\gamma$, e^+e^-, or $\mu^+\mu^-$), followed by final states with a γ and a meson and by two-meson final states.

In terms of a constituent quark model the radiative annihilations $p\bar{p} \rightarrow \gamma X$ most likely imply the destruction of a colour-singlet quark–antiquark pair with $J^{PC} = 1^{--}$. In the Vector Meson Dominance model (VMD) this transition is related to the sum of amplitudes with the same quark–antiquark pair arranging itself into a real vector meson ρ or ω. Only one phase is free in this relation and can be determined from the comparison of the radiative branching ratios with the corresponding two-meson branching ratios.

There has previously been a lack of observations of radiative $p\bar{p}$ annihilations, with the only observed reaction being $p\bar{p} \rightarrow \gamma\pi^0$ [1, 2]. Therefore, using the Crystal Barrel detector at LEAR, we have made a systematic study of reactions of the type

$$p\bar{p} \rightarrow \gamma X \ , \tag{1}$$

where $X = \gamma$, π^0, η, ω, and η'. This investigation was made possible by the excellent electromagnetic calorimetry of the Crystal Barrel detector, i.e. its nearly hermetic solid-angle coverage and very good energy and spatial resolution for photons, and by the large amount of data taken with an open (minimum-bias) and a specific (zero-prong) trigger.

The detector covers 98% of the full solid angle and is sensitive both to charged particles and photons. Charged particles are detected in two proportional wire chambers (PWCs) and a cylindrical jet drift chamber (JDC). Single photons and photons produced by the decays of mesons ($\pi^0 \rightarrow \gamma\gamma$, $\eta \rightarrow \gamma\gamma$, $\omega \rightarrow \pi^0\gamma$, etc.) are measured in the electromagnetic calorimeter which surrounds the drift chamber. The detector is placed in a solenoidal magnet providing a field of 1.5 T. The low-energy antiprotons (beam momentum 200 MeV/c) enter the detector along the field axis, are detected by a segmented silicon counter just in front of the liquid hydrogen target, and are stopped in the target. As the results presented here rely primarily on the calorimeter, we briefly describe its relevant characteristics. A detailed description of the apparatus is given elsewhere [3].

The calorimeter consists of 1380 CsI(Tl) crystals, 16 radiation lengths thick, read out by photodiodes. The crystals point towards the target centre; they cover polar angles between 12° and 168° and have complete coverage in azimuth. The energy calibration of the crystals is obtained using the 2γ decay of the π^0, abundantly produced in $p\bar{p}$ annihilations, by imposing the standard mass of 134.97 MeV/c^2 on the reconstructed π^0. The photon energy resolution varies slightly from run to run and is

$$\frac{\sigma_E}{E_\gamma} = \frac{2.6\%}{(E_\gamma/\mathrm{GeV})^{1/4}} \tag{2}$$

for the data used in this work. The angular resolution in both the polar and the azimuthal angle ($\sigma_{\theta,\phi}$) varies with the photon energy from 20 to 35 mrad for isolated showers and is about 35 mrad for two or more showers in the same cluster of crystals.

Data taken with two different trigger settings have been used in the present analysis: i) 3.9 million 'minimum-bias' events were taken with an open trigger where the detector

is read out every time a $\bar{p}$ enters the target; these were analysed to provide an absolute normalization for the branching ratios of reactions (1), choosing as the reference reaction $p\bar{p} \to \pi^0\pi^0$;
ii) 4.5 million '0-prong' events, which were taken with a trigger requiring that there are no charged particles in the final state, using on-line information provided by the PWC and JDC. The enrichment factor of this trigger is 28. These data were used to determine relative branching ratios with small statistical errors. The sample of 4.5×10^6 0-prong events corresponds to 107×10^6 $p\bar{p}$ annihilations at rest.

We next describe the cuts applied to the 0-prong data sample in order to select specific final states. The sample is first scanned to eliminate residual events with charged tracks in either the PWC or JDC which had not been recognized by the trigger. This reduces the sample to 4.15×10^6 good 0-prong events. Since we wish to analyse fully contained events, we then reject all events where one or more photons hit the rings of crystals adjacent to the beam entrance and exit holes because part of the shower energy may have leaked out. The next cut selects the desired number of photons in the final state. One photon may deposit energy in as many as 30 crystals. The reconstruction program determines clusters as groups of neighbouring crystals with energy deposits larger than 1 MeV. The total energy of the cluster must be at least 10 MeV. If the cluster contains only one local maximum it is considered a single particle-energy-deposition (PED). The PED energy is the sum of the energy deposits in the individual crystals and its direction is the energy-weighted average direction of the crystals. If there are, however, more than one, say n, local maxima in a cluster, one PED is associated with each such maximum, and the total cluster energy is partitioned between the n PEDs according to

$$E^i_{PED} = \frac{E^i_9}{\sum_i E^i_9} \cdot E_{cluster} \tag{3}$$

with $i = 1, ..., n$; E^i_9 is the sum of energies over the 3×3 crystal matrix centred on the ith local maximum, which is assumed to be the impact point of the shower.

The number of PEDs is identified with the number of electromagnetic showers, i.e. photons in the final state. Figure 1 shows a three-dimensional plot of a 3-PED event. It is a $\pi^0\gamma$ event with an almost symmetrical π^0 decay. The two γ's have merged into one cluster for this smallest possible laboratory angle between two γ's from a meson decay. Two effects may lead to misidentification of events. One is the loss of one or more photons, either by dead regions of the detector or by the energy threshold of 10 MeV. The other is the occurrence of additional PEDs due to shower fluctuations – called 'split-offs'. Split-offs are characterized by their small energy and their proximity to a higher energy PED. Both effects are well understood. They are reproduced by Monte-Carlo-simulated showers using the program GEANT [4] and are included in the detection efficiency for good events and the feedthrough (i.e. misidentification) probabilities for background events.

The possible misidentification of events requires a simultaneous treatment of the wanted channels and potential background channels. Hence the following event topologies were analysed: 2 PEDs ($\gamma\gamma$), 3 PEDs ($\pi^0\gamma, \eta\gamma, \eta'\gamma$), 4 PEDs ($\pi^0\pi^0, \eta\pi^0, \eta'\pi^0$, $\omega\gamma$), and 5 PEDs ($\omega\pi^0$). For each event topology we impose energy and momentum conservation by applying a four-constraint (4C) kinematic fit to the hypothesis $p\bar{p} \to \gamma_1, .., \gamma_n$, n being the observed number of photons (PEDs). We reject events with a confidence level less than 15% in the confidence level distribution which is flat for values above 10%.

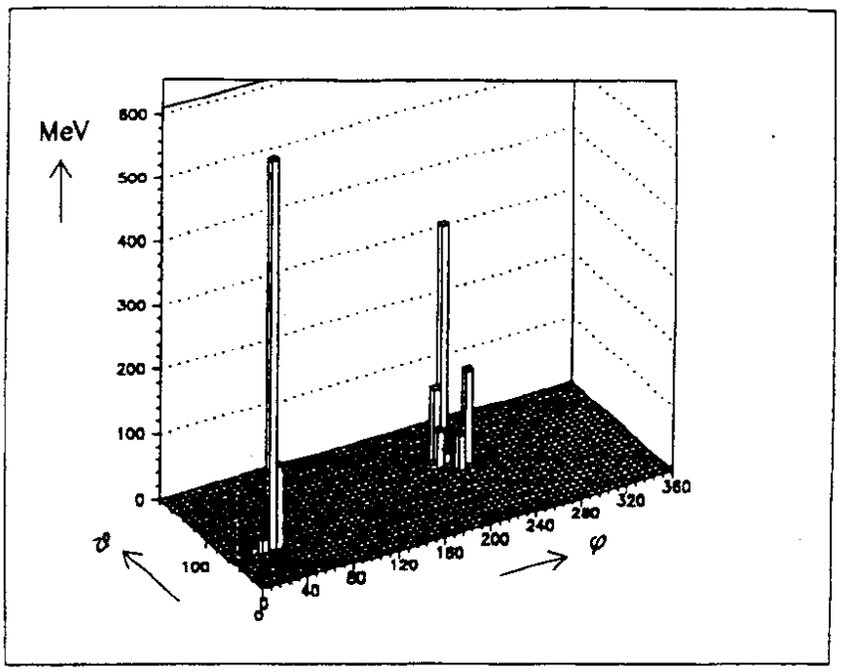

Figure 1: Three-dimensional plot of a 3-PED event. The vertical coordinate represents the energy deposit in a crystal, and the horizontal coordinates are the polar angle θ and azimuthal angle ϕ.

Once an n-PED channel has been selected, the presence of a particular reaction is established by reconstructing the meson(s) involved. We identify π^0, η, and η' mesons in their 2γ-decay mode by calculating the invariant mass of all possible $\gamma\gamma$ combinations in an event. This is shown in Figs 2a and b for 3- and 4-PED events where π^0 and η peaks can easily be identified. (The remaining, flat background is almost purely combinatorial). The ω meson is identified by its $\pi^0\gamma$ decay mode. Figure 2c gives the invariant $\pi^0\gamma$ mass for four-photon events. If the invariant mass is within a 3σ window of the mass given in the Review of Particle Properties [5], the event is considered as originating from the corresponding meson. The experimental widths of the invariant mass distributions depend weakly on the energies of the mesons. The following values are the experimental widths (σ in MeV) of the mass peaks for the reactions studied in this work: (9.7 ± 0.2), (15.7 ± 0.7), (18.2 ± 0.6), and (19.5 ± 3.2) for π^0, η, ω, and η', respectively. Finally, a 5C kinematic fit is applied to the channels $\gamma\pi^0$, $\gamma\eta$, $\gamma\eta'$, and a 6C kinematic fit to the channels $\pi^0\pi^0$, $\eta\pi^0$, $\eta'\pi^0$, requiring in all cases a fit probability of at least 15% to accept the event. The number of ω mesons is determined by fitting the peak with a Gaussian and a polynomial background. As an example, we list the number of events retained after each step of the sequence of cuts for the channel $\pi^0\gamma$: topology cut (3 PEDs) and 4C kinematic fit: 4302 events; 3σ window on $\gamma\gamma$ mass: 2889 events; 5C kinematic fit(hypothesis $\pi^0\gamma$): 2867 events.

The detection efficiencies are determined by a complete Monte Carlo (MC) simulation based on GEANT [4] taking into account all the cuts applied to the real data. Similarly, all the feedthrough probabilities from a physical channel into neighbouring topologies (e.g. the probability that a real $\pi^0\gamma$ event is identified as a $\gamma\gamma$ event after having lost a photon) are determined.

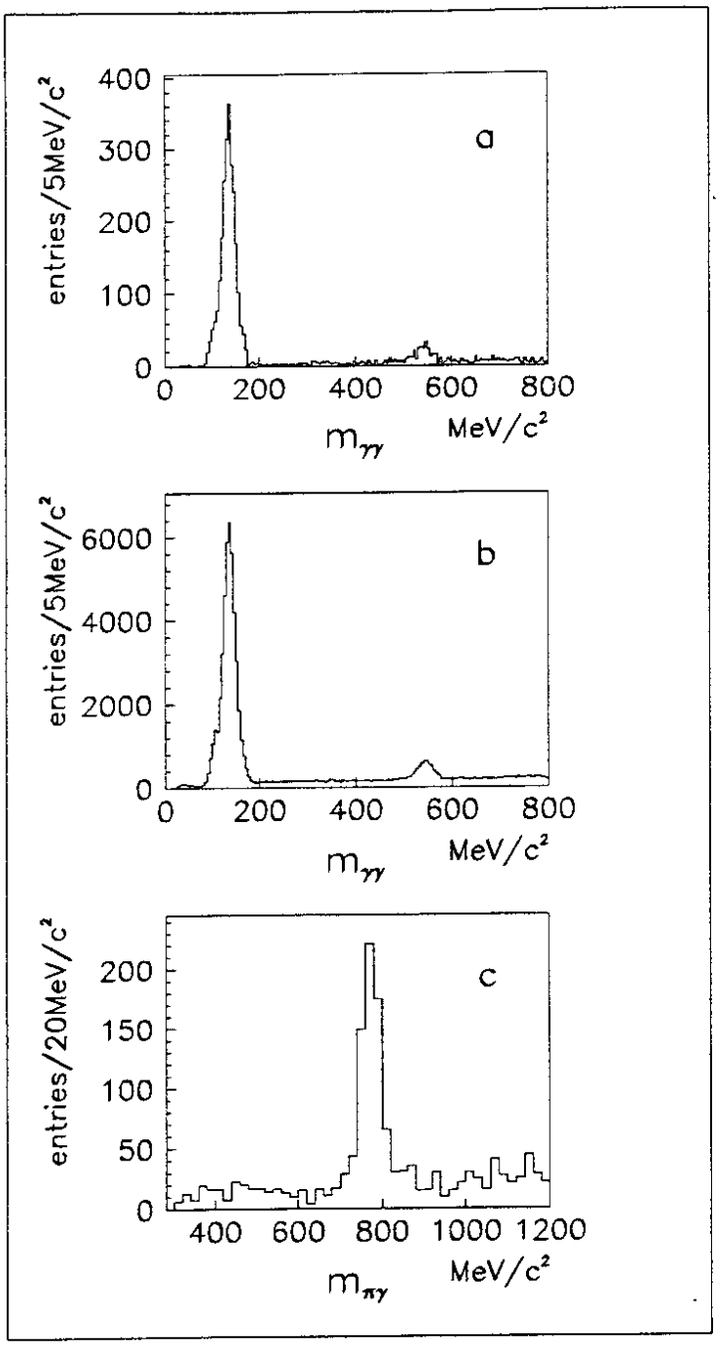

Figure 2: The invariant two-photon mass spectrum obtained for a) three-photon events (3 entries per event); b) four-photon events (4 entries per event); c): The invariant $\pi^0\gamma$ mass spectrum from four-photon events for those γ's which do not combine with the remaining (fourth) γ to a π^0, η or η' within the 3σ windows.

Examples for the distribution of the measured γ and π^0 momenta of $\gamma\gamma$, $\pi^0\gamma$, and $\pi^0\pi^0$ events surviving all the cuts are shown in Fig. 3. The momentum distributions still contain the background from feedthrough mentioned above which has to be subtracted. As an example for the background calculation we consider again the channel $\pi^0\gamma$. The observed $\pi^0\gamma$ events contain a background of $\pi^0\pi^0$ events where one photon was lost and which the 4C kinematic fit cannot distinguish from true $\pi^0\gamma$ events. Thus the feedthrough is mainly due to the loss of a low-energy photon which did not pass

the 10 MeV energy threshold. If higher energy photons are lost the event is rejected by the energy or momentum conservation requirement. Feedthrough from the other side, $\gamma\gamma$ events, via split-off photons is negligible owing to the low rate of $\gamma\gamma$ events. From the observed number of $\pi^0\pi^0$ events the number of background events in the $\pi^0\gamma$ sample can be calculated using the detection efficiency for the $\pi^0\pi^0$ channel and the feedthrough probability from the $\pi^0\pi^0$ to the $\pi^0\gamma$ channel. As a result, we found that the percentage of true $\pi^0\gamma$ events is $(66 \pm 3)\%$ of the observed signal. We checked this result by comparing the π^0 momentum distributions for $\pi^0\gamma$ and $\pi^0\pi^0$ events (Figs. 3b and c).

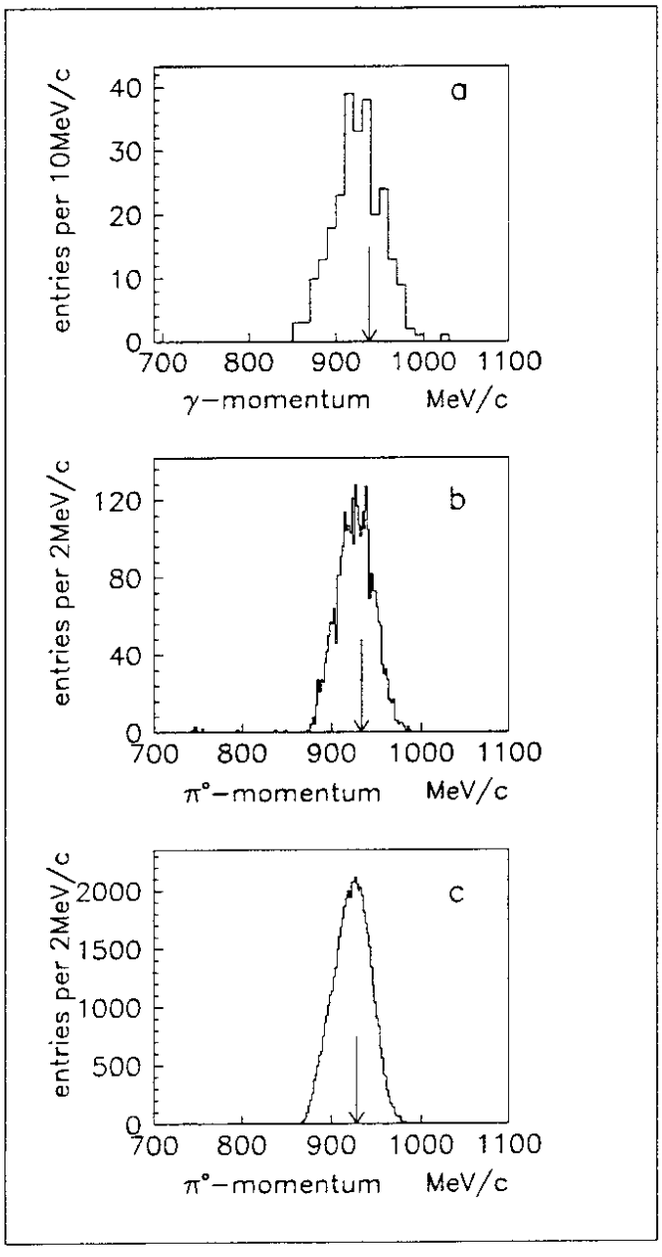

Figure 3: Momentum distributions for single photons and pairs of photons. The measured momenta are used for events passing all the cuts including kinematic fits. Theoretical values are indicated by arrows. a): The γ momentum distribution for two-photon events passing the 4C fit. b): The π^0 momentum distribution in $\pi^0\gamma$ events passing the 5C kinematic fit. c): The π^0 momentum distribution in $\pi^0\pi^0$ events passing the 6C kinematic fit.

The expected π^0 momenta are 933.42 and 928.51 MeV/c for true $\pi^0\gamma$ and $\pi^0\pi^0$ events, respectively, and their difference is 4.91 MeV/c. The measured average momenta are 926.0±0.4 and 922.5±0.1 MeV/c, respectively. The $\pi^0\pi^0$ events are practically background free and we attribute the discrepancy of 0.6% between expected and average measured momenta to a systematic error in the energy calibration. As the nominal π^0 momentum for $\pi^0\pi^0$ events we thus take the average measured momentum (922.5 MeV/c) and for the true $\pi^0\gamma$ events we assume it to be $922.5 + 4.9 = 927.4$ MeV/c. Supposing that the shift of 1.4 MeV/c of the π^0 momentum relative to this nominal momentum in $\pi^0\gamma$ is caused by the background of $\pi^0\pi^0$, we can determine the relative amount of the background. By this method the percentage of true $\pi^0\gamma$ events is found to be $(71 \pm 8)\%$ in good agreement with the value derived via the method described before.

The annihilation channels investigated in this work are listed in Table 1, together with the number of observed events, the detection efficiency, and the number of events from the dominant background channels. The number of background events was calculated as described above for the $\pi^0\gamma$ example, from three input numbers: i) the number of events observed in the correct topology (e.g. 4 PEDs for $\pi^0\pi^0$); ii) the detection efficiency found by the MC simulation for the correct topology, and iii) the feedthrough probability to the wrong topology, found by the MC simulation. The errors represent statistical uncertainties.

Table 1: Number of events observed in 4.5×10^6 0-prong events, detection efficiency, and calculated number of background events contained in the observed events. For the channels $\gamma\gamma$ and $\eta'\gamma$ an enlarged event sample of 6×10^6 events was used.

Final state	Number of observed events	Efficiency (%)	Number of background events
$\pi^0\pi^0$	25910 ± 161	(35.7 ± 0.2)	
$\pi^0\gamma$	2867 ± 54	(40.6 ± 0.3)	$\pi^0\pi^0$: 974 ± 43
$\eta\pi^0$	2765 ± 53	(31.5 ± 0.4)	
$\eta\gamma$	281 ± 18	(38.9 ± 0.6)	$\pi^0\eta$: 67 ± 7 $\pi^0\pi^0$: 21 ± 6 $\pi^0\gamma$: 44 ± 4
$\omega\pi^0$	15064 ± 203	(27.9 ± 0.3)	
$\omega\gamma$	387 ± 38	(22.8 ± 0.3)	$\pi^0\omega$: 248 ± 27
$\eta'\pi^0$	128 ± 14	(45.3 ± 0.5)	
$\eta'\gamma$	11 ± 3	(35.6 ± 0.3)	$\eta'\pi^0$: 3 ± 1 $\pi^0\gamma$: 1 ± 1
$\gamma\gamma$	98 ± 10	(54.1 ± 0.4)	$\pi^0\gamma$: 54 ± 5 $\pi^0\pi^0$: 16 ± 6

Studies of possible systematic errors of the MC efficiency were performed by varying cuts for real data and MC events. Variation of the effective solid angle and the confidence level cut of the 4C fit led to a variation of the branching ratio of 2.1% and 1.5%, respectively. Split-offs and missing photons were searched for in data and MC simulated $\pi^0\pi^0$ events and were reproduced by the simulation within 2%. The loss of low-energy photons was quantitatively studied using a large data sample of $\pi^0\omega$ events. 22112 ± 296 complete (5-PED) events were found and 544 ± 52 4-PED events with a missing low energy photon can be identified in the invariant $\gamma\gamma$ mass distribution where a clear ω signal shows up. From this ratio we conclude that the feedthrough probability is $544 \times 0.279/22112 = 0.69 \pm 0.06\%$ (where 0.279 is the $\pi^0\omega$ efficiency in 5 PEDs). A MC generated sample of $\pi^0\omega$ events yielded for the feedthrough probability $0.75 \pm 0.03\%$ in good agreement with the experimental number. Hence we conclude that the systematic error on the feedthrough probability is smaller than the statistical error, see Table 1. The photon energy threshold was varied between 10 and 20 MeV, which led to a variation of the branching ratio of 2.8%. We also introduced a vertex shift of 5 mm in the MC simulation to study the influence on the efficiencies of a possible vertex shift in the real data. This caused a change in the efficiency of 3%. From these studies we derive a relative systematic error of 5.5% for our efficiency assuming the various systematic errors are uncorrelated.

In order to obtain absolute branching ratios for the reactions of Table 1, we have used $p\bar{p} \to \pi^0\pi^0$ as the reference reaction. Therefore, a second analysis was performed for this reaction on the basis of the minimum-bias data set with 3.9 million events. Applying the same cuts as for the 0-prong data we find 866 ± 29 $\pi^0\pi^0$ events. The fraction of antiprotons not stopping in the target was determined to be $(3.9 \pm 0.7)\%$, and the fraction of events with annihilation occurring in flight $(5.7 \pm 1.1)\%$. Applying these corrections to the number of antiprotons and using the efficiency for the $\pi^0\pi^0$ channel of Table 1 we calculate the branching ratio for $\pi^0\pi^0$ to be $(6.82 \pm 0.46) \times 10^{-4}$. This number is in good agreement with another, partly independent, analysis of our data [6] which gave $(6.93 \pm 0.43) \times 10^4$. The $\pi^0\pi^0$ branching ratio is then used to normalize the 0-prong data set to the minimum-bias data set, and the absolute branching ratios for the other channels can be calculated.

The branching ratios are listed in Table 2 together with the results of previous measurements [1, 7]. We also list our results for the channels $\pi^0\pi^0$, $\eta\pi^0$, $\eta'\pi^0$, and $\omega\pi^0$ which

Table 2: Resulting branching ratios and phases between the I = 0 and I = 1 amplitude

Channel	This experiment	Previous measurements	cos β
$\pi^0\gamma$	$(44 \pm 4) \times 10^{-6}$	$(17.4 \pm 2.2) \times 10^{-6}$ [1]	-0.75 ± 0.11
$\eta\gamma$	$(9.3 \pm 1.4) \times 10^{-6}$	$\leq 8.7 \times 10^{-5}$(95% CL) [7]	-0.78 ± 0.25
$\omega\gamma$	$(68 \pm 19) \times 10^{-6}$	$\leq 9.6 \times 10^{-4}$(95% CL) [7]	-0.60 ± 0.18
$\eta'\gamma$	$\leq 12 \times 10^{-6}$(95% CL)	$\leq 2.0 \times 10^{-4}$(95% CL) [7]	
$\gamma\gamma$	$\leq 0.63 \times 10^{-6}$(95% CL)	$\leq 1.7 \times 10^{-6}$(95% CL) [1]	
$\pi^0\pi^0$	$(6.9 \pm 0.4) \times 10^{-4}$[6]	$(2.06 \pm 0.14) \times 10^{-4}$ [1]	
$\eta\pi^0$	$(2.12 \pm 0.12) \times 10^{-4}$[6]	$(1.33 \pm 0.27) \times 10^{-4}$ [1]	
$\omega\pi^0$	$(57 \pm 5) \times 10^{-4}$[6]	$(52 \pm 5) \times 10^{-4}$ [9]	
$\eta'\pi^0$	$(1.23 \pm 0.13) \times 10^{-4}$[6]	$(5 \pm 2) \times 10^{-4}$ [9]	

were analysed in this work because they contribute to the background. The measurement and analysis of these reactions is described in more detail in two separate publications [6, 8]. The branching ratios for the latter reactions represent a cross check for our method since they can be compared with previous measurements [1, 9]. The branching ratios include all decay modes of the two final-state particles, not just those observed in this experiment. The branching ratios for the specific decays of π^0, η, η', and ω used to identify these particles were taken from the Review of Particle Properties [5]. The errors in Table 2 include statistical errors of the signal and background, of the MC calculated detection efficiencies and feedthrough probabilities, and the errors of tabulated meson decays [5]; they include as well all the systematic errors mentioned above for the detection efficiencies, feedthrough probabilities and the reference $\pi^0\pi^0$ branching ratio.

For the channel $p\bar{p} \rightarrow \pi^0\gamma$ two measurements already exist [1, 2]. The more precise one [1] is inconsistent with our measurement. It should be noted that a similar discrepancy exists for the channel $\pi^0\pi^0$ measured by the same experiment [1]. A broad and intensive search for a possible error in our data or analysis has been unsuccessful. The branching ratios for the channels $p\bar{p} \rightarrow \gamma\gamma$, $\eta\gamma$, and $\omega\gamma$ have been measured for the first time in this work and lie typically an order of magnitude below previous upper limits. For $p\bar{p} \rightarrow \eta'\gamma$ we measure a new upper limit which is more than a factor of ten smaller than the previous one. Since the $\gamma\gamma$-signal has only a statistical significance of two standard deviations, $(0.33 \pm 0.15) \times 10^{-6}$, we prefer to give an upper limit (0.63×10^{-6}).

In the Vector Meson Dominance model (VMD) these branching ratios are related to branching ratios for final states with one of the vector mesons replacing the photon (see Fig. 4). As an example, the branching ratio $BR_{\pi^0\gamma}$ of $p\bar{p} \rightarrow \pi^0\gamma$ is related to $BR_{\pi^0\rho}$ and $BR_{\pi^0\omega}$ by the following expression from Ref. [10],

$$\frac{BR_{\pi^0\gamma}}{P_{\pi^0\gamma}} = g^2_{\gamma\rho}\left[\frac{BR_{\pi^0\rho^0}}{P_{\pi^0\rho^0}} + \frac{BR_{\pi^0\omega}}{9P_{\pi^0\omega}} + \frac{2}{3}\cos(\beta)\sqrt{\frac{BR_{\pi^0\rho^0}BR_{\pi^0\omega}}{P_{\pi^0\rho^0}P_{\pi^0\omega}}}\right] \tag{4}$$

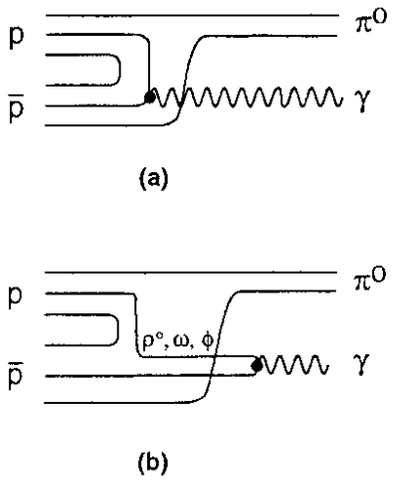

Figure 4: a): An example of a quark line diagram for the radiative annihilation $p\bar{p} \rightarrow \pi^0\gamma$. b): The corresponding quark line diagrams in the VMD for the isospin I = 0 ($\rho\pi^0$) and I = 1 ($\omega\pi^0$ or $\phi\pi^0$) amplitudes.

where P_x is the kinematic partial width (centrifugal barrier penetration factor times two-body phase space) for the relevant decay. We use those given by von Hippel and Quigg [11]. β is the phase between the amplitude for the intermediate $\pi^0\rho$ (I = 0) and that for $\pi^0\omega$ (I = 1) from the $^3S_1$ $p\bar{p}$ initial state (assuming that only this initial state contributes). $g_{\gamma\rho}$ is the $\gamma\rho^0$ coupling constant with $g^2_{\gamma\rho} = 3 \times 10^{-3}$ [10]. In this relation the amplitudes to final states containing a ϕ meson are being neglected since they are relatively small. Similar expressions hold for the other channels. In the case of $\gamma\gamma$ and $\gamma\omega$ the dominant initial $p\bar{p}$ state is assumed to be $^1S_0$ and the phase β refers to this state.

To calculate the predictions of the VMD we use the measured branching ratios for $p\bar{p} \to \pi^0\rho$ [7], $\pi^0\omega$, $\eta\omega$, $\omega\omega$ [8], $\eta\rho$ [1], $\omega\rho$ [12], $\rho\rho$ [13]. Our results for the branching ratios of radiative annihilations all lie well within the range predicted by the VMD if we take as upper and lower limits those values obtained for $\cos(\beta) = \pm 1$ in relation (4). These limits are, for instance, 3.8×10^{-5} and 8.6×10^{-5} for $\pi^0\gamma$, and 7.1×10^{-8} and 6.9×10^{-7} for $\gamma\gamma$. The measured values are in most cases close to the lower limit. In other words, extracting the only free parameter, the phase β, from the above relation between measured branching ratios we find that the interference is close to maximally destructive, $\cos(\beta)$ near -1 for all channels except $\gamma\gamma$.

We also compare our measured γX branching ratios with the following naïve estimate, which in contrast to the VMD does not make any assumptions on the intermediate states but directly relates final-state photon emission to π^0 emission. Since the phase space of both particles is about equal we assume that the γX branching ratio is smaller than the $\pi^0 X$ branching ratio by a factor equal to the fine structure constant α, but is favoured by an inverse suppression factor $(f_P)^{-1}$, relative to those channels ($\pi^0\pi^0$ and $\eta\pi^0$) which can only be produced from P-states of protonium. The suppression factor f_P is the fraction of P-state annihilation to all annihilations (S plus P) which we assume to be around 15%; see also Ref. [6]. Thus we expect the ratios $BR_{\pi^0\gamma}/BR_{\pi^0\pi^0}$, $BR_{\eta\gamma}/BR_{\eta\pi^0}$, and $BR_{\eta'\gamma}/BR_{\eta'\pi^0}$ to be of the order $\alpha/f_P = 4.9\%$. The experimental values are $(6.5 \pm 0.4)\%$, $(4.4 \pm 0.6)\%$, and $\leq 12\%$ respectively. For the ratios $BR_{\omega\gamma}/BR_{\omega\pi^0}$ and $BR_{\gamma\gamma}/B_{\gamma\pi^0}$ we expect a value around $\alpha = 0.73\%$: the experimental values are $(1.1 \pm 0.3)\%$ and $\leq 1.4\%$, respectively. Given the simplicity of the estimate the agreement with the measurement turns out to be surprisingly good.

We wish to thank the technical staff of the LEAR machine group and of all the participating institutions for their invaluable contributions to the success of the experiment. We acknowledge financial support from the German Bundesministerium für Forschung und Technologie, the Schweizerischer Nationalfonds, the British Science and Engineering Research Council, and the U.S. Department of Energy (contract Nos. DE-FG03-87ER40323 and DE-AC03-76SF00098). J.K. and K.M.C. acknowledge support from the A. von Humboldt Foundation. We also wish to thank K. Steinberger and N. Gollwitzer for the system management on the computer cluster in Garching.

References

[1] L. Adiels et al., Z. Phys. **35** (1987) 15.

[2] G. Backenstoss et al., Nucl. Phys. **228B** (1983) 424.

[3] E. Aker et al., Nucl. Instrum Methods **A321** (1992) 69.

[4] R. Brun et al., GEANT3, Internal Report CERN DD/EE/84-1 (1987).

[5] K. Hikasa et al., Phys. Rev. **D45**, No.11 (1992) Part II, Review of Particle Properties.

[6] C. Amsler et al., Phys. Lett. **B297** (1992) 214.

[7] M. Chiba et al., Phys. Rev. **D38** (1988) 2021.

[8] C. Amsler et al., Antiproton–proton annihilation at rest into two-body final states, accepted for publication in Z. Phys. C.

[9] M. Chiba et al., Phys. Lett. **B202** (1988) 447.

[10] B. Delcourt, J. Laysec and E. Pelaquier, Proc. Workshop on Physics at LEAR with Low Energy Antiprotons, Erice, 1982 (Plenum, New York, 1984).

[11] F. v. Hippel and C. Quigg, Phys. Rev. **D5** (1972) 624.

[12] R. Bizzari et al., Nucl. Phys. **B14** (1969) 169.

[13] J. Diaz et al., Nucl. Phys. **B16** (1970) 239.